Graphical Abstract

Computational exploration of α-lactone rearrangements and the cyclic halonium zwitterion from bromination of acrylate anion in water: implicit vs. explicit solvation.

John H. Glancy, Marcus S. Lewis and Ian H. Williams
Department of Chemistry, University of Bath, Bath, UK BA2 7AY

Leave this area blank for abstract info.

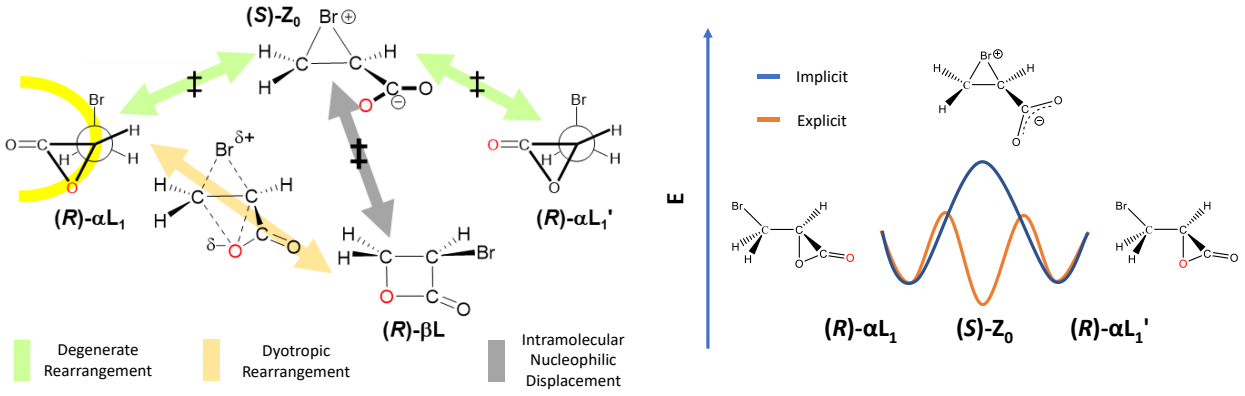

Tetrahedron
journal homepage: www.elsevier.com

Computational exploration of α-lactone rearrangements and the cyclic halonium zwitterion from bromination of acrylate anion in water: implicit *vs.* explicit solvation.

John H. Glancy, Marcus S. Lewis and Ian H. Williams

Department of Chemistry, University of Bath, Bath, UK BA2 7AY

ARTICLE INFO

Article history:
Received
Received in revised form
Accepted
Available online

Keywords:
α-Lactone
Rearrangement
Implicit and explicit solvation
Free-energy profile

ABSTRACT

In memory of Jonathan Williams, a valued colleague of incisive intellect (and regarded by undergraduates as 'the better-looking Prof. Williams' in the Department).

Bromomethyloxiranone has a much larger repertoire of molecular acrobatics than previously recognised: conformational isomerism, degenerate rearrangement that exchanges O atoms in the α-lactone ring, and epimerisation, all of which occur with lower barriers than dyotropic rearrangement to the more stable β-lactone. DFT calculations (B3LYP/6-31+G*) with implicit solvation (PCM) by water predict the cyclic bromonium zwitterion (formally derived from addition of Br^+ to acrylate anion) to be a transition structure but QM/MM simulations, combining the same DFT method with explicit solvation by many MM water molecules and using molecular dynamics to obtain free-energy profiles and surfaces, reconfirms the status of the cyclic bromonium as an intermediate.

1. Introduction

Halolactonisation is the well-known synthetic procedure whereby electrophilic halogenation of an unsaturated carboxylic acid yields a lactone product.[1] The mechanism is generally considered to involve initial formation of an intermediate cyclic halonium ion which then undergoes intramolecular nucleophilic substitution with the carboxyl group attacking the halonium moiety. For example, Rousseau and co-workers [2] reported the preparation of α-bromo-β-lactones by use of bis(collidine) bromine(I) hexafluoro-phosphate in DCM as the electrophilic reagent with β-substituted α,β-unsaturated acids. With R = H and R′, R″ = alkyl or with R = alkyl, R′ = aryl, R″ = H (Scheme 1), the process may be represented as a 4-exo-tet cyclisation with attack of the carboxylate group on a cyclic bromonium ion. When R, R″ = H and R′ = aryl the intermediate is believed to be a resonance-stabilised benzylic cation which undergoes decarboxyation. With R, R″ = H and R′ = alkyl, polymeric products were reported which were considered to arise from the intermediacy of a highly reactive α-lactone.

α-Lactones are Cinderella species, whose existence is often overlooked. However, we have presented experimental evidence for the intermediacy of an α-lactone in the aqueous bromination of 2,3-dimethylmaleate and fumarate dianions (**1** and **4**) at room temperature [3]: the stereochemistry of each specific bromo-β-lactone product (**3** or **6**), as determined unambiguously by X-ray crystallography, is most economically rationalised by a mechanism in which an α-lactone (**2** or **5**) is the first-formed intermediate (Scheme 2).

We have also reported density-functional theoretical (DFT) results within the polarised continuum model (PCM) of aqueous solvation indicating that addition of Br^+ to acrylate anion led directly to a bromomethyl-α-lactone [4]. The cyclic bromonium zwitterion $\mathbf{Z_0}$ was found to be a transition structure (TS) for a degenerate rearrangement of the α-lactone (Scheme 3, $\boldsymbol{\alpha L_1' \rightarrow Z_0 \rightarrow \alpha L_1}$) that exchanges the two oxygen atoms of the carboxylate group (coloured black and red). Whereas in principle one would imagine that the carboxylate nucleophile in $\mathbf{Z_0}$ could attack either C_α or C_β leading to an α-lactone or β-lactone **βL**, respectively, in practice this competition did not exist since $\mathbf{Z_0}$ was not an intermediate at the B3LYP/6-31+G* level with implicit solvation by water. A TS (corresponding to a first-order saddle point) can connect only two valleys which, in this case, are those for $\boldsymbol{\alpha L_1'}$ and $\boldsymbol{\alpha L_1}$.

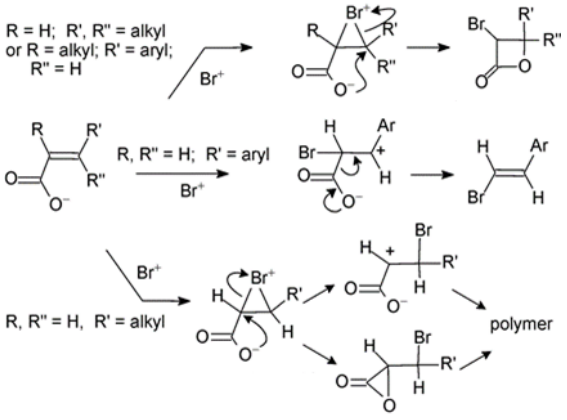

Scheme 1.

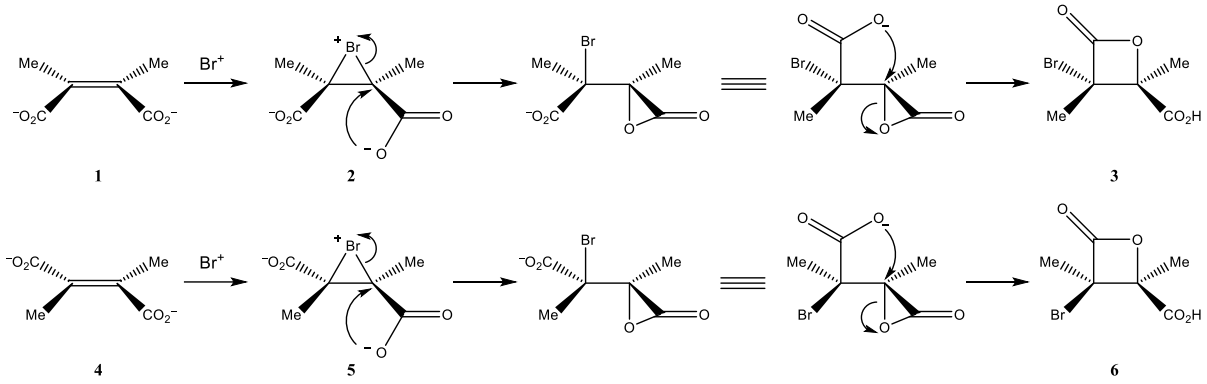

Scheme 2.

In this paper we present new B3LYP/6-31G*/PCM results for implicit solvation by water that greatly expand the picture previously presented and demonstrate the amazing agility of these bromo-α-lactones in molecular acrobatics involving not only the degenerate rearrangement mentioned above but also conformational isomerisation, epimerisation and dyotropic rearrangement. Moreover, we show how a hybrid quantum-mechanics/molecular-mechanics (QM/MM) method, using B3LYP/6-31G* in combination with a classical potential (TIP3P) for explicit solvation by water, predicts the cyclic bromonium zwitterion to be a discrete intermediate after all. This example serves to illustrate the limitation of the PCM method for describing molecular species that, while being neutral overall, contain separated charges. The QM/MM work involves molecular dynamics (MD) simulations from which free-energy profiles (1D) and surfaces (2D) may be obtained, allowing for more reliable computational exploration of mechanisms for organic reactions in solution.

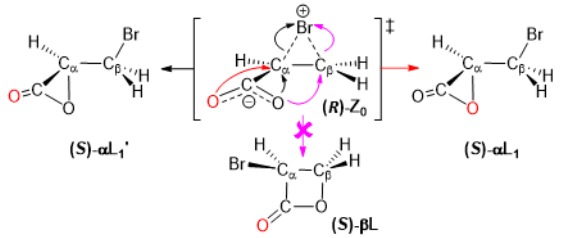

Scheme 3.

2. Results and Discussion

2.1. Implicit solvation with B3LYP/6-31+G/PCM*

Scheme 4 shows a topological map of pathways for α-lactone rearrangements in water based on B3LYP/6-31+G*/PCM relative energies. The zero of energy is the α-lactone conformer of lowest energy, denoted by a subscript$_0$; this conformer has the C=O and C_β–Br bonds in a nearly antiperiplanar arrangement, as depicted by the Newman projection. Red and black colour is used (as above) to distinguish the two O atoms whose positions are exchanged by the degenerate rearrangement: a prime is used to denote a species with a "red" carbonyl O. The α-lactones exist in enantiomeric series, and so the species shown in the top-right corner of Scheme 4 is labelled as **(*S*)-αL$_0$′**. The next lowest conformer is **(*S*)-αL$_1$′** and its congeners, in which the C=O and C_β–Br bonds lie in roughly perpendicular planes, and the C_α–O and C_β–Br bonds are approximately antiperiplanar; this conformer is just 0.8 kJ mol^{-1} above the one of lowest energy. The third rotamer **(*S*)-αL$_2$′**, etc., is 2.6 kJ mol^{-1} higher than that of lowest energy. The three conformers are interconnected by rotation about the C_α–C_β bond and each pair is separated by a TS, the relative energy of which is shown in square brackets; the subscript shows the magnitude of the wavenumber/cm^{-1} corresponding to the imaginary frequency for vibrational motion across the barrier. All six species lie on a closed pathway shown by the yellow loop.

According to the B3LYP/6-31+G*/PCM method, the degenerate rearrangement (*cf.* Scheme 3 and the green double-headed arrow in Scheme 4) interconnects **(*S*)-αL$_1$′** and **(*S*)-αL$_1$** (as well as **(*R*)-αL$_1$′** and **(*R*)-αL$_1$**): this pathway involves neighbouring-group participation (NGP) by Br towards C_α coupled with C_α–O bond cleavage and rotation about the C_α–CO_2 bond. The cyclic bromonium species is the lowest-energy zwitterion on the map (hence the labels **(*S*)-Z$_0$** and **(*R*)-Z$_0$**) and has atoms $C_\beta C_\alpha CO_2$ approximately coplanar and perpendicular to the plane $C_\beta C_\alpha$Br. Depending on whether a clockwise or anticlockwise rotation occurs, either of the two O atoms may reform the C_α–O bond of the α-lactone.

Epimerisation at C_α occurs by means of acyclic zwitterions **Z$_1$**, **Z$_2$** and **Z$_3$** which are TSs lying on the pathways delineated by the pink and violet double-headed arrows. In these species the two O atoms are more-or-less symmetrically disposed either side of the $C_\beta C_\alpha C$ plane, and the vibrational motion across each barrier is a rocking of the CO_2 group to either side of that plane. NGP does not occur because nucleophilic approach of Br is repelled by one of the negative-charged O atoms. **(*R*$_a$)-Z$_1$** and **(*S*$_a$)-Z$_1$** each show axial chirality, whereas **Z$_2$** and **Z$_3$** are achiral. The **Z$_1$** and **Z$_2$** TSs each interconnect different conformers of enantiomeric α-lactones, as well as interchanging the O atoms; their relative energies are similar and a little higher than that of **Z$_1$** due to the absence of stabilisation from NGP. **Z$_3$** offers a higher-energy pathway between enantiomers of the lowest-energy α-lactone rotamer.

Two more acyclic and achiral zwitterions **Z$_4$** and **Z$_5$** are very high-energy TSs that interconvert the two enantiomers of **Z$_0$** by means of anti- and synperiplanar arrangements of the atoms Br$C_\beta C_\alpha CO_2$, as shown by the blue double-headed arrows. These pathways involve coupled rotations about the C_α–C_β and C_α–CO_2 bonds.

Finally, the α-lactone may undergo a dyotropic rearrangement to form the more stable β-lactone; this involves concerted intramolecular nucleophilic substitution at the vicinal C_α and C_β atoms, as previously described for chloromethyloxiranone [5]. This may occur from any of the **αL$_1$** species, in which the C_α–O and C_β–Br bonds are approximately antiperiplanar; Scheme 4 shows pathways (buff-coloured double-headed arrows) from **(*S*)-αL$_1$′** and **(*R*)-αL$_1$** species but omits those from **(*S*)-αL$_1$** and **(*R*)-αL$_1$′** to save space. Since the barrier to dyotropy is significantly higher than any of the barriers for degenerate rearrangement or epimerisation, let alone conformational isomerisation, of the α-

lactone, all these processes may occur many times before the α-lactone rearranges to the β-lactone.

It is clear that the B3LYP/6-31+G*/PCM method predicts all of the charge-separated, zwitterionic species to be of higher energy than the α- and β-lactones comprised only of all covalent bonds, even though the C_α–O bond in an α-lactone has considerable ionic character [6]. But does this method, involving implicit solvation by a continuum dielectric medium, provide an accurate description of charge-separated species, even though they are neutral overall? That is the question that must now be addressed by means of a method involving explicit solvation by many discrete water molecules, which will allow specific solute-solvent hydrogen-bonding interactions; the QM/MM approach is well suited for this purpose, albeit at very much greater computation cost. The next section considers results for some of the key species and pathways discussed above.

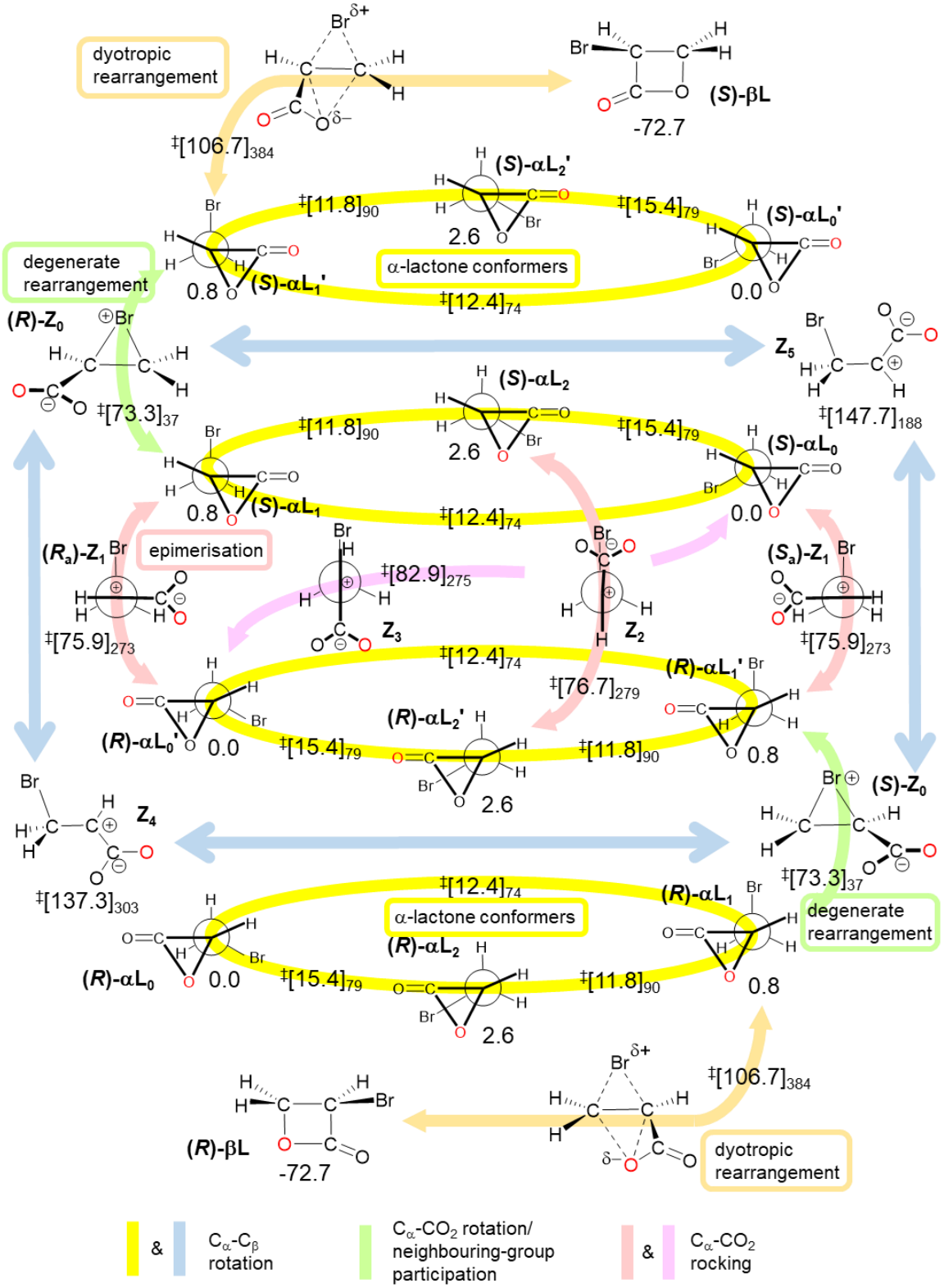

Scheme 4. Topological map of pathways for α-lactone rearrangements in water based on B3LYP/6-31+G*/PCM relative energies for implicit solvation.

2.2. Explicit solvation with B3LYP/6-31G/TIP3P*

Replacing the structureless dielectric continuum of the PCM implicit solvation model by an explicit solvent box containing 1034 water molecules described by a classical potential, allows for re-evaluation of the average structures and relative energies of the species depicted in Scheme 4. Moreover, free-energy differences may be estimated for individual mechanistic pathways, by methodology that takes into account not only the effects of temperature (corresponding to experimental conditions) but also of specific hydrogen-bonding interactions between solute and solvent. Although in real water the α-lactone rearrangements would occur in competition with hydrolysis, the use of a molecular mechanics description (TIP3P) for water in these simulations precludes this possibility. Full details of the calculations are provided in the Computational Methods section.

The relative energies of the predominantly covalent α-lactone structures and of the β-lactone are not greatly affected by either implicit (PCM) or explicit (QM/MM) solvation, as expected. However, the energies of the zwitterions relative to the lactones is likely to be underestimated by PCM owing to the omission of specific hydrogen bonds involving water molecules and the carboxylate group. Most of the pathways shown in Scheme 4 are not affected greatly by the change from an implicit to an explicit model for solvation, and so are not considered here. The question of particular interest for this work concerns the nature of the cyclic bromonium zwitterion **Z₀**: is it a TS or an intermediate? Does it lie at a saddle point on the free-energy surface or in an energy well?

Figure 1 shows a 1D free-energy profile for the dyotropic rearrangement of **(*S*)-αL₁′** to **(*S*)-βL** at 300 K. Each point corresponds to the potential of mean force averaged over many configurations from a MD trajectory for the QM solute in MM solvent, and with the difference of distances (C_α–O) – (C_β–O) constrained to a particular value. The predicted barrier height appears to be greater than that found with implicit solvation, but care should be exercised because there is no guarantee that the chosen reaction coordinate drives the 1D profile through the real saddle point on the multidimensional free-energy hypersurface. The key point is that the pathway for dyotropic rearrangement exists within the explicit solvation model.

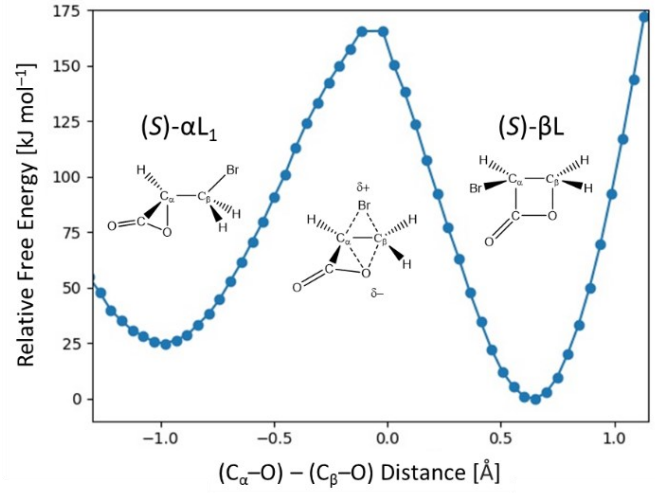

Figure 1. Relative free-energy profile for dyotropic rearrangement of α-lactone to β-lactone (B3LYP/6-31+G*/TIP3P) in explicit water.

Figure 2 shows a 1D free-energy profile for conversion of **(*R*)-βL** to **Z₀** at 300 K, obtained in a similar manner but with the C_β–O distance alone as the reaction coordinate. The maximum in this profile corresponds to a transition state distinct from that for the dyotropic rearrangement but clearly similar in structure. Both involve attack on the C_β by the same oxygen; however, the average value of the (C_α–O) – (C_β–O) difference of distances (the reaction coordinate used in Figure 1) for representative structures at the maximum of Figure 2 is -1.17 Å. This is in contrast to the value of ca. 0.1 Å for the dyotropic rearrangement maximum in Figure 1, showing that these are two distinct maxima on the free energy hypersurface. One can rationalise the higher-energy dyotropic rearrangement as an almost lateral transfer of the α-lactone oxygen from C_α to C_β, whereas the lower energy, intramolecular nucleophilic displacement maximum (Figure 2) involves a 4-exo-tet cyclisation by the carboxylate group on the cyclic bromonium.

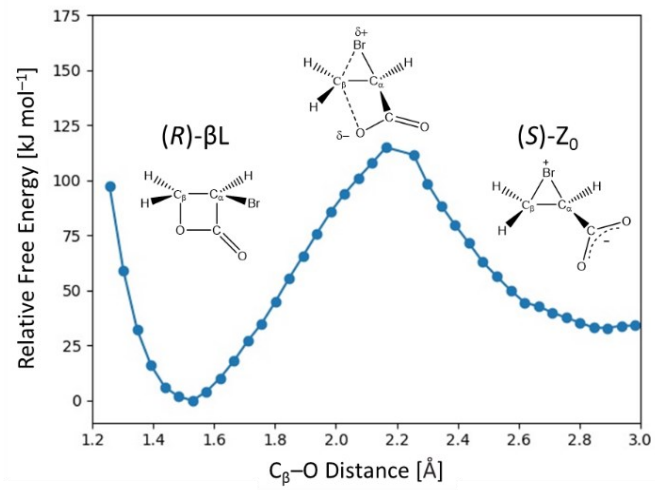

Figure 2. Relative free-energy profile for conversion of β-lactone to cyclic bromonium zwitterion (B3LYP/6-31G*/TIP3P) in explicit water.

The key point, however, is that the cyclic bromonium zwitterion lies in a free-energy minimum, meaning that it is an intermediate and not a transition state within the explicit solvation model. (Note that a saddle point on a free-energy hypersurface, averaged over many configurations of a condensed-phase system, corresponds to a transition state, whereas a saddle point on a potential-energy surface for a single configuration corresponds to a transition structure [7].)

Figure 3 shows the first solvation shell for representative structures of both a charge-separated zwitterionic species (**(*S*)-Z₀**), and a non-charge-separated α-lactone species (**(*S*)-αL₁**). What is clear from Figure 4 is that the oxygens in the carboxyl substituent in **Z₀** are involved in many more explicit solvent-solute interactions than the oxygens in the α-lactone and that the H-bonding distance in these interactions are, on average, shorter for the zwitterionic species. This figure illustrates how specific solute-solvent interactions simulated through explicit solvation can greatly reduce the energy of a charge-separated structure, relative to a non-charge-separated species.

Figure 4 shows a 2D free-energy surface for conversion of α-lactone **(*R*)-αL₂** to **Z₀** at 300 K as a function of two reaction coordinates, the C_α–O and C_α–Br distances. Of note are the free energy minima corresponding to **(*R*)-αL₂**, **(S)-Z₀**, and **(*S*)-αL₂**, which is accessed from **(*R*)-αL₂** *via* a C_α–CO_2 rocking motion similar to that described in Scheme 4. The key point again is that the cyclic bromonium zwitterion lies in a free-energy minimum. It appears to be lower in energy than the α-lactone but once again this may be an artefact due to the constraints placed upon the reaction coordinates: the limited sampling of configurational space may not have been sufficient to give adequate statistical

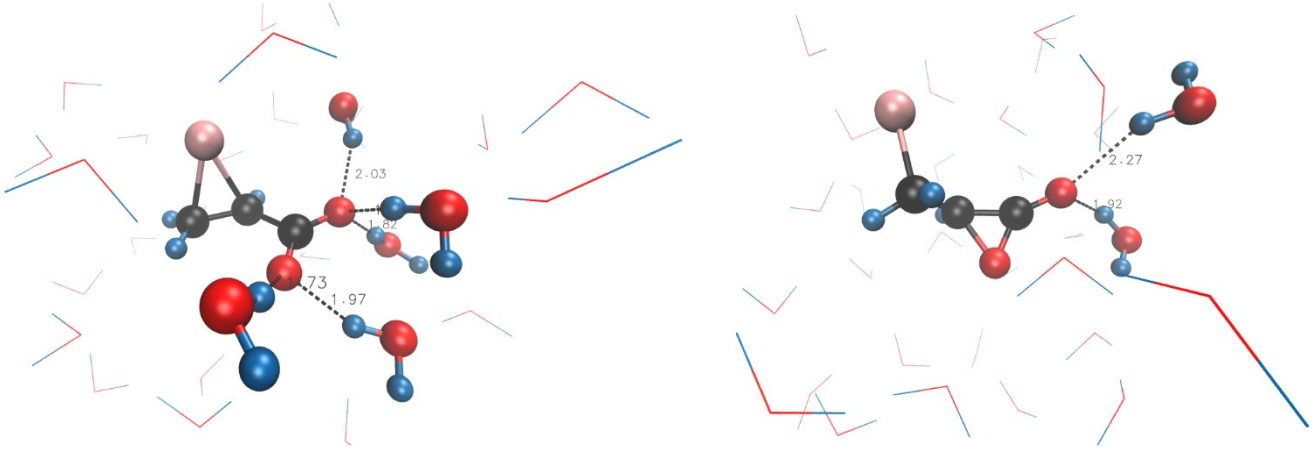

Figure 3. First solvation shells for the charge-separated **(*S*)-Z₀** (left) and the non-charge-separated **(*S*)-αL₁** (right) with solute-solvent hydrogen-bonding interactions under 2.2 Å highlighted. Representative structures were extracted from the equilibration MD trajectory.

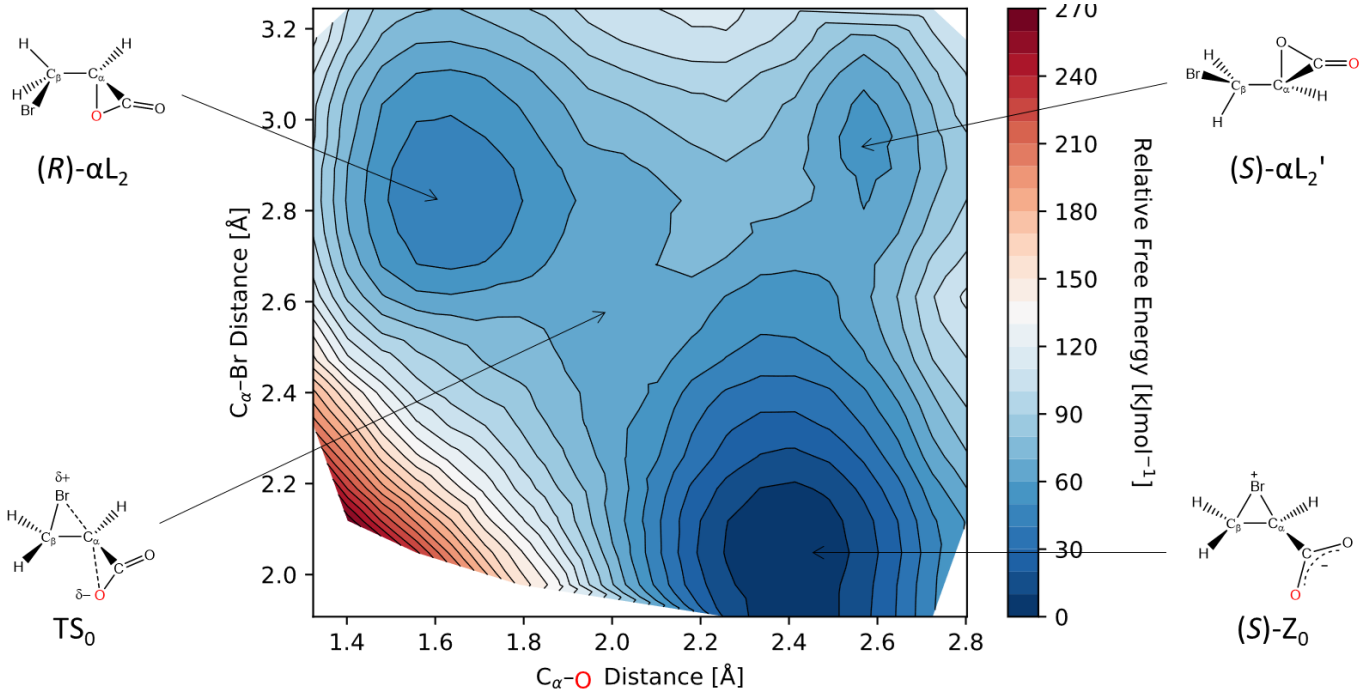

weight to regions of the multidimensional hypersurface as projected onto the reduced dimensionality 2D surface shown here. Also of note is the general smoothness of the free energy surface in the region of the **(*R*)-αL₂** minimum. While the mechanism involves a transition state for intramolecular nucleophilic displacement (**TS₀**) and likely goes through the **(*R*)-αL₁** conformer, the representative structure found in the α-lactone free energy well is that of **(*R*)-αL₂**. This suggests that, in explicit solvation, the **(*R*)-αL₂** conformer is the most stable, with little to no barrier between conformers along the reaction coordinate. This could be due to the larger dipole moment of the **(*R*)-αL₂** conformer being favourably solvated by the explicit solvent or the donation of electron density into the carbonyl carbon by bromine, leading to partial negative charge build-up on the carbonyl oxygen, which would also be more strongly solvated by the explicit hydrogen bonding network.

Whichever order the α-lactone and cyclic bromonium zwitterion's true energies are found to lie in, Figure 4 shows that using an explicit solvation method greatly reduces the difference in energy between the two. It also shows that they both occupy free energy minima on the free energy hypersurface, separated by a transition state that represents an intramolecular nucleophilic displacement (**TS₀**), in this model of the system.

2.3. Relation to experiment and role of solvent dynamics

There is growing experimental evidence that some reactions, which would previously have been considered as proceeding by means an ion-pair intermediate, involve reorganisations that occur too rapidly to be accounted for by a stepwise mechanism. For example, Richard and co-workers have reported the solvolysis of optically pure 1-(3-nitrophenyl)ethyltosylate in 50/50 (v/v) trifluoroethanol/water: compound with ^{18}O in each of the non-bridging position in the tosylate group undergoes degenerate rearrangement, to exchange the isotopic label with ^{16}O originally connected to the benzylic C atom, 80 times faster than racemisation (epimerisation) and 10 times faster than would be predicted if both processes occurred by partitioning of a common ion-pair intermediate.[8-10] The pathway for this rearrangement was described as "uncoupled concerted",[11] where "concerted" refers to the absence of an intermediate and "uncoupled" indicates that C-^{16}O bond breaking, reorganization of the tosylate group, and C-^{18}O bond making occur as essentially independent processes.[8,9] These experiments are beautifully designed to explore "borderline" mechanisms and, although some might regard this type of detailed investigation of "simple" reactions disdainfully as a trivial pursuit, they shed light on the

fascinating subtlety of chemical behaviour and expose the limits of our understanding of supposedly well-known reactions. However, they also point to the complementary role of computational simulation, especially where solvent dynamics may dictate the outcomes of reactions that traverse free-energy landscapes on which the existence of intermediates with finite vibrational lifetimes and lying in energy wells is uncertain.

Singleton has recently shown that the products of HCl addition to 1,3-pentadiene cannot be explained simply by means of the carbocation (from initial protonation) partitioning as a solvent-equilibrated intermediate in a free-energy well; some product also results from non-equilibrated "intermediate", and depends critically upon solvent dynamics.[12] Furthermore, computational modelling of this system in nitromethane has demonstrated the inadequacy of implicit solvation methods and the usefulness of dynamical trajectory calculations with explicit solvation.[12]

These studies indicate the relevance and significance of our computational explorations of α-lactone rearrangements. These involve zwitterionic species as possible intermediates or transition states, whereas the reactions studied by these other authors involve ion pairs, but the similarities are striking. Moreover, these other works serve to reinforce our emphasis on the importance of explicit solvation models and point the way forward to further QM/MM MD studies of the influence of solvent dynamics on these intriguing reactions (*cf.* ref 13.

3. Computational Methods

3.1. QM methods

All optimisations were performed by means of the GAUSSIAN16 program [14] using the B3LYP density functional method [15] with the 6-31+G* basis [16] (with six Cartesian d functions on non-hydrogen atoms), together with the PCM method [17] for aqueous solvation using ε = 78.4 and default UFF radii for the molecular cavity. Convergence in the SCF procedure was typically achieved using the "very tight" option; geometry optimisations used default convergence criteria. TSs were located by means of QTS2, QTS3 and EF methods as appropriate, and were characterised as possessing a single imaginary frequency corresponding to the transition vector (or reaction coordinate mode) for a particular chemical transformation, in contrast to energy minima with all-real vibrational frequencies. Single-point *in vacuo* energies were evaluated with Cartesian coordinates for optimised structures without PCM.

3.2. QM/MM methods

QM/MM molecular dynamics calculations were performed by means of the fDynamo library [18]. Structures were optimised using the QM optimisation method outlined above and then added to a 31.4 Å cubic box of 1034 pre-equilibrated water molecules. Any waters with an oxygen atom lying within a radius of 2.8 Å from an atom of the solute were removed. The MM subsystem was described by the TIP3P [19] potential within the OPLS-AA force field [20]. For each structure, the QM system was frozen, and the MM subsystem was equilibrated for 1000 ps using a time-step of 1 fs with classical Langevin-Verlet MD. This was conducted at 300 K in the NVT ensemble with periodic boundary conditions.

3.3. Potentials of Mean Force (PMFs)

One-dimensional potentials of mean force (1D-PMFs) were constructed by averaging the atomic motions of the whole system at 300 K, as governed by the QM/MM potential energy function and forces for a QM solute (described using the B3LYP/6-31+G* functional/basis set pair) surrounded by a 31.4 Å box of TIP3P water molecules. Residues containing an atom within 15 Å of any atom of the solute, excluding solute, were included in the MM environment. Solute and MM environment atoms were free to move while all other atoms in the system remained frozen. The value of the reaction coordinate was incremented along 20 simulation windows, using umbrella sampling with a harmonic constraint of 2500 kJ mol^{-1} Å^{-2}. For each window, a Langevin-Verlet MD (300 K, NVT) simulation was undertaken comprising 300 fs of equilibration, followed by a 1.2 ps production trajectory (time-step = 1 fs), from which the PMF was obtained by means of the weighted-histogram analysis method (WHAM) [21].

A two-dimensional potential of mean force (2D-PMF) was constructed in a similar fashion to the 1D-PMF method but with respect to two reaction coordinates (C_α–O and C_α–Br distance), using double umbrella sampling in 13 x 13 simulation windows as previously described [13].

4. Conclusions

QM/PCM studies at the B3LYP/6-31+G* level of theory have shown that bromomethyloxiranone can access a much larger array of distinguishable structural arrangements than previously recognised. These include conformational isomerism, degenerate rearrangement that exchanges O atoms in the α-lactone ring, and epimerisation; all of which occur with lower barriers than dyotropic rearrangement to the more stable β-lactone.

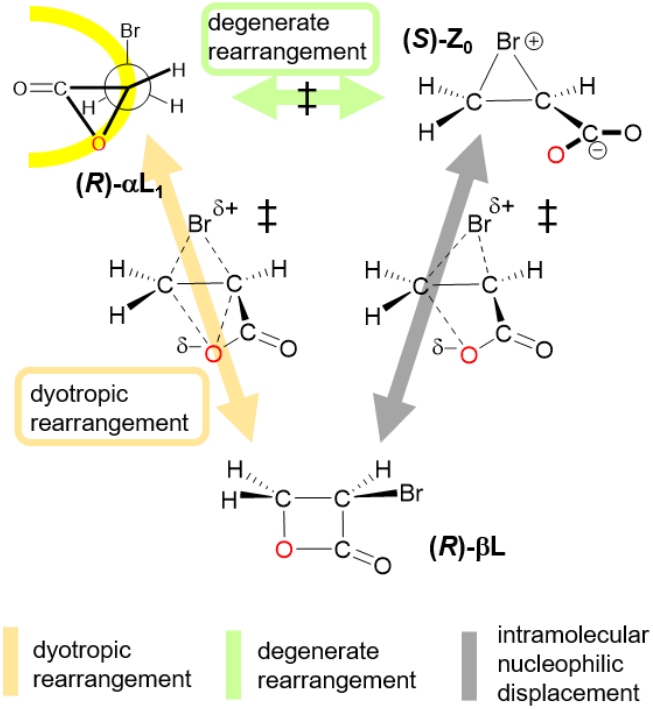

Scheme 5.

This work has also sought to highlight the how important the effect of solvent environment is on the calculations of even simple organic mechanisms. Use of the widely employed IEFPCM model [11], when coupled with the B3LYP/6-31+G* functional/basis set pair, predicts that the cyclic bromonium zwitterion **Z$_0$** is located at a first-order saddle point, ca. 70 kJ mol^{-1} higher in energy than **αL$_0$** and is in fact the transition state for degenerate rearrangement of the α-lactone **αL$_1$**. Explicit solvation using the same quantum mechanical method with a molecular mechanical treatment of the solvent (TIP3P), on the other hand, locates the cyclic bromonium zwitterion in a free energy minimum at similar energies to those of the α-lactone species. This method would suggest that the cyclic bromonium zwitterion is a true intermediate in this mechanism and similar in

energy to the α-lactone species. The relative heights of free energy maxima along the three intramolecular rearrangements shown in Scheme 5 suggest that intramolecular nucleophilic displacement from cyclic bromonium zwitterion to **βL** would outcompete dyotropic rearrangement from **αL** to **βL**.

This work aims to highlight the effect that differing solvation systems can have on calculated results. Explicit solvation leads to more numerous and stronger hydrogen-bonding interactions between solvent molecules and the carboxylate group in $\mathbf{Z_0}$, than between solvent molecules and the same oxygens in non-charge-separated species. This is predicted to be the driving force in reducing the energy gap between $\mathbf{Z_0}$ and the lactone species.

5. Acknowledgements

This work was supported by the EPSRC Centre for Doctoral Training in Sustainable Chemical Technologies (Studentship to J.H.G.) and made use of the Balena High Performance Computing (HPC) Service at the University of Bath.

6. References

[1] (a) S. Ranganathan, K. M. Muraleedharan, N. K. Vaish, N. Jayaraman, Tetrahedron 60 (2004) 5273-5308; (b) M. D. Dowle, D. I. Davies, Chem. Soc. Rev. 8 (1979) 171-197.

[2] (a) F. Homsi, G. Rousseau, J. Org. Chem. 64 (1999) 81-85; (b) S. Robin, G. Rousseau, Eur. J. Org. Chem. (2002) 3099-3114.

[3] (a) J. J. Robinson, J. G. Buchanan, M. H. Charlton, R. G. Kinsman, M. F. Mahon, I. H. Williams, Chem. Commun. (2001) 485 –486.; (b) N. Pirinççioğlu, J. J. Robinson, M. F. Mahon, J. G. Buchanan, I. H. Williams, Org. Biomol. Chem. 5 (2007) 4001-4009.

[4] G. D. Ruggiero, I. H. Williams, Chem. Commun. (2002) 732-733.

[5] J. G. Buchanan, G. D. Ruggiero, I. H. Williams, Org. Biomol. Chem. 6 (2008) 66 – 72.

[6] J. G. Buchanan, M. H. Charlton, M. F. Mahon, J. J. Robinson, G. D. Ruggiero, I. H. Williams, J. Phys. Org. Chem. 15 (2002) 642-646.

[7] I. Tuñón, I. H. Williams, Adv. Phys. Org. Chem. **53** (2019) 29-68.

[8] Y. Tsuji, M. M. Toteva, T. L. Amyes, J. P. Richard, Org. Lett. **6** (2004) 3633-3636.

[9] Y. Tsuji, J. P. Richard, Chem. Record **5** (2005) 94-106.

[10] Y. Tsuji, J. P. Richard, J. Amer. Chem. Soc. **128** (2006) 17139-17145.

[11] W. P. Jencks, Chem. Soc. Rev. **10** (1981) 345-375.

[12] V. A. Roytman, D. A. Singleton, J. Amer. Chem. Soc. **142** (2020) 12865-12877.

[13] Gaussian 16, Revision C.01, M. J. Frisch, G. W. Trucks, H. B. Schlegel, G. E. Scuseria, M. A. Robb, J. R. Cheeseman, G. Scalmani, V. Barone, G. A. Petersson, H. Nakatsuji, X. Li, M. Caricato, A. V. Marenich, J. Bloino, B. G. Janesko, R. Gomperts, B. Mennucci, H. P. Hratchian, J. V. Ortiz, A. F. Izmaylov, J. L. Sonnenberg, D. Williams-Young, F. Ding, F. Lipparini, F. Egidi, J. Goings, B. Peng, A. Petrone, T. Henderson, D. Ranasinghe, V. G. Zakrzewski, J. Gao, N. Rega, G. Zheng, W. Liang, M. Hada, M. Ehara, K. Toyota, R. Fukuda, J. Hasegawa, M. Ishida, T. Nakajima, Y. Honda, O. Kitao, H. Nakai, T. Vreven, K. Throssell, J. A. Montgomery, Jr., J. E. Peralta, F. Ogliaro, M. J. Bearpark, J. J. Heyd, E. N. Brothers, K. N. Kudin, V. N. Staroverov, T. A. Keith, R. Kobayashi, J. Normand, K. Raghavachari, A. P. Rendell, J. C. Burant, S. S. Iyengar, J. Tomasi, M. Cossi, J. M. Millam, M. Klene, C. Adamo, R. Cammi, J. W. Ochterski, R. L. Martin, K. Morokuma, O. Farkas, J. B. Foresman, and D. J. Fox, Gaussian, Inc., Wallingford CT, 2016.

[14] (a) A.D. Becke, J.Chem.Phys. 98 (1993) 5648-5652. (b) C. Lee, W. Yang, R.G. Parr, Phys. Rev. B 37 (1988) 785-789. (c) S.H. Vosko, L. Wilk, M. Nusair, Can. J. Phys. 58 (1980) 1200-1211. (d) P.J. Stephens, F.J. Devlin, C.F. Chabalowski, M.J. Frisch, J.Phys.Chem. 98 (1994) 11623-11627.

[15] (a) R. Ditchfield, W. J. Hehre, J. A. Pople, J. Chem. Phys., 54 (1971), 724. (b) W. J. Hehre, R. Ditchfield, J. A. Pople, J. Chem. Phys., 56 (1972), 2257. (c) P. C. Hariharan, J. A. Pople, Theor. Chem. Acc., 28 (1973), 213-22. (d) P. C. Hariharan, J. A. Pople, Mol. Phys., 27 (1974), 209-14. (e) M. S. Gordon, Chem. Phys. Lett., 76 (1980), 163-68. (f) M. M. Francl, W. J. Pietro, W. J. Hehre, J. S. Binkley, D. J. DeFrees, J. A. Pople, M. S. Gordon, J. Chem. Phys., 77 (1982), 3654-65. (g) R. C. Binning Jr., L. A. Curtiss, J. Comp. Chem., 11 (1990), 1206-16. (h) J.-P. Blaudeau, M. P. McGrath, L. A. Curtiss, L. Radom, J. Chem. Phys., 107 (1997), 5016-21. (i) V. A. Rassolov, J. A. Pople, M. A. Ratner, T. L. Windus, J. Chem. Phys., 109 (1998), 1223-29. (j) V. A. Rassolov, M. A. Ratner, J. A. Pople, P. C. Redfern, L. A. Curtiss, J. Comp. Chem., 22 (2001), 976-84. (k) T. Clark, J. Chandrasekhar, G. W. Spitznagel, P. v. R. Schleyer, J. Comp. Chem., 4 (1983), 294-301.

[16] J. Tomasi, B. Mennucci, R. Cammi, Chem. Rev., 105 (2005), 2999-3093.

[17] M. J. Field, M. Albe, C. Bret, F. Proust-De Martin, A. Thomas, J. Comput. Chem. **21** (2000), 1088-1100.

[18] W. L. Jorgensen, J. Chandrasekhar, J. D. Madura, R. W. Impey, M. L. Klein. J. Chem. Phys. **79** (1983), 926−935.

[19] M. J. Robertson, J. Tirado-Rives, W. L. Jorgensen, J. Chem. Theory Comput., 11 (2015), 3499-3509.

[20] S. Kumar, D. Bouzida, J. Comput. Chem. **13** (1992), 1011-1021.

[21] J. J. Ruiz-Pernía, I. Tuñón, I. H. Williams. J. Phys. Chem. B **114** (2010), 5769-5774.